UDC 666-492:666.762.1:548.4

PARAMAGNETIC DEFECTS IN ALUMINUM OXIDE NANOPOWDERS AND CERAMICS BASED ON THESE POWDERS

V. S. Kiiko,[1] E. V. Zabolotskaya,[1] L. V. Zolotukhina,[1] N. M. Frolov,[1] I. A. Dmitriev,[1] and Yu. N. Makurin[1]

The defective structure of aluminum oxide nanopowders and ceramics based on these powders is analyzed using the electron paramagnetic resonance method. Inherent structural point defects, which are oxygen vacancies having a trapped electron (F^+ centers), are identified in the nanopowders. Among the impurity defects, the signals of Fe^{3+}, Cr^{3+}, and Ti^{3+}, which occupy different crystallographic positions in Al_2O_3 or exist as separate phases, are identified in the nanopowders and ceramics.

Nanopowders and ceramics based on nanopowders are of special interest for the practice and theory of materials science. The average size of the microcrystals in such powders ranges from 12 to 100 nm and in ceramics, from 100 to 350 nm. Nanopowders, as a rule, are characterized by a phase composition that is not traditional for the particular material and is metastable under normal conditions.

The interest in the nanostructural state of powders is determined by the influence of the size effects on a number of physicochemical and technological properties of powders. Numerous publications in the last decade discussed the production of nanopowders and nanopowder ceramics [1 – 3]. Due to the controlled growth of grains in powders and ceramics, it becomes possible to study the regularities of the formation of inherent and impurity defects, the contribution of the defective inter-crystallite surface phase to the overall defectiveness of the material, the inherent luminescence centers, as well as the effect of the size and the degree of perfection of the nanocrystals on the mechanical, luminescent, and exothermic emissive properties.

At present, Al_2O_3 single crystals treated in a reducing medium at various temperatures are successfully applied as the working medium in thermoluminescent sensors for ionizing radiation. One of the promising lines in the development and upgrading of sensors consists in the development of new types of working media for solid-body detectors based on dense light-transmitting aluminum oxide ceramics. The use of nanodimensional powder as initial material for producing high-density transmitting aluminum oxide ceramics makes it possible to improve the optical quality and sensitivity of the detectors and thus to increase the efficiency and reliability of registered dosimetric data. We have established that the introduction of TiO_2 into aluminum oxide ceramics makes it possible to substantially increase the peak intensity of thermally stimulated luminescence, due to defects caused by the impurity titanium ions in the forbidden zone of Al_2O_3. At the same time, the defect structure of Al_2O_3 nanopowders produced by different methods (wire explosion or laser evaporation of ceramics), as well as aluminum oxide ceramics made of nanopowders with or without titanium dioxide additive, remains unstudied. In this context, the study of the defect structure of nanopowders and ceramics based on nanopowders is of special importance.

The studies were performed on nanodimensional pure Al_2O_3 powders, powders with TiO_2 additives in the amount of 0.3, 1.0, and 2.5 wt.%, and ceramics made from the above powders using magnetic-pulse compression and subsequent sintering in accordance with a special technology [3].

The Al_2O_3 nanopowders were obtained by two methods. At the Electrophysical Institute of the Ural Branch of the Russian Academy of Sciences, the powders were produced at the Pulse Process Laboratory by electrical explosion of wires made of pure aluminum and metallic titanium.[2] The mixtures of aluminum oxide nanopowder with titanium dioxide additives were prepared by joint mixing of powder suspensions in isopropyl alcohol with ultrasonic field superposition until thickening [2, 3]. Next, the mixture was dried and pulverized. The main physicochemical and technological properties of these powders and ceramics based on them are shown in Tables 1 and 2.

All Al_2O_3 powders have weakly expressed nanocrystal morphology. The spherical shape prevails.

---

[1] Ural State Technical University, Ekaterinburg, Russia; Institute of Chemistry of Solids, Ural Branch of the Russian Academy of Sciences, Ekaterinburg, Russia.

[2] Samples for the studies were supplied by Yu. A. Kotov and V. V. Ivanov.

TABLE 1

Nanopowder	Phase composition, wt.%	Specific surface area, m²/g	Average crystal size,[*] nm	Density, g/cm³
Al_2O_3	$80\delta + 20\gamma$ $\leq 1\alpha, \theta$	59	28	0.08
TiO_2	22 rutile + 78 anatase	69	54	0.14
Al_2O_3 + 0.3 wt.% TiO_2	Al_2O_3: $20\gamma + 80\delta$	75	–	0.49
Al_2O_3 + 1.0 wt.% TiO_2	TiO_2: 25 ana- tase + 75 rutile	76	–	0.49
Al_2O_3 + 2.5 wt.% TiO_2		76	–	0.49

[*] According to x-ray analysis data.

TABLE 2

Chemical composition of ceramics, wt. %	Sintering temperature, K	Sintering duration, min	Density of ceramics, g/cm³	Average crystal size in ceramics,[*] nm
Al_2O_3	1633	4	3.84	140 – 180
Al_2O_3 + 0.3 wt.% TiO_2	1683	19	3.84	> 200
Al_2O_3 + 1.0 wt.% TiO_2	1683	6	3.81	> 200
Al_2O_3 + 2.5 wt.% TiO_2	1683	–	–	> 200

[*] According to x-ray analysis data.

The nanopowders (produced by explosions) of pure Al_2O_3 and Al_2O_3 with TiO_2 additives were used to make ceramic samples. Their phase composition is represented by the stable modification α-Al_2O_3 and TiO_2 in the form of rutile.[2]

We obtained Al_2O_3 nanopowders through evaporation of aluminum oxide ceramics, employing a solid-body pulse laser beam on yttrium aluminum garnet activated by Nd^{3+} ions ($\lambda = 1.064$ μm).

The average radiation power of the YAG laser (modulation of the factor of merit for pulse repetition frequency 25 ± 5 kHz) constituted 16 ± 3.2 W. The aluminum oxide powders produced by laser evaporation differ in their phase composition from the nanopowders produced by electric explosion. The analysis of their phase composition indicated that approximately 80% is represented by γ-phase, and the second phase can be presumably attributed to ε-type. Judging by the x-ray diffraction patterns, the Al_2O_3 microcrystals in the nanopowders are poorly formed.

The chemical composition of the initial aluminum oxide ceramics which was used to obtain a nanopowder through evaporation indicated the presence of iron impurities in the amount of 0.02 – 0.09 wt.%. It can be expected that the nanopowder as well contains iron impurity, whose amount is close to the initial content.

For comparison, a nanopowder was produced by electric explosion of iron wire. The phase composition of the nanopowder determined by x-ray analysis was as follows (wt.%): 97.0 γ-Fe_2O_3, < 1.0 Fe_3O_4, 2.0 α-Fe_2O_3. The powder had a specific surface area of about 16 m²/g and density 4.6 – 4.8 g/cm³. The average microcrystal size calculated on the basis of x-ray measurements was $\approx$ 80 nm.

The electron radiation of the samples was carried our in air using a Radan-220 pulse accelerator with the following electron beam parameters: electron energy 200 keV, current density $\approx$ 100 A/cm², pulse duration $\approx$ 3 nsec. The exposure dose was $\approx 5.0 \times 10^5$ R.

The paramagnetic defects in the nanopowders and the nanopowder-based ceramics were investigated employing an ERS-200 electron paramagnetic resonance (EPR) spectrometer in the x-ray range at room temperature (Table 3).

The spectra of the nanopowders produced by both methods exhibit two signals (I and II), which have different field positions, bandwidth, and intensity (Fig. 1). The weaker signal I correlates with Fe^{3+} ions, which are capable of isomorphically replacing Al^{3+} ions in the cation sublattice of Al_2O_3. The registered value of the g-factor is typical of Fe^{3+} in an octahedral crystalline field with strong orthorhombic distortion [4].

The shape of the line of signal II indicates that this is the superposition of two wide signals. One of them presumably corresponds to iron ions in a different crystallographic environment. To verify this assumption, an EPR spectrum of the nanopowder produced by iron wire explosion was taken. It

TABLE 3

| Sample	Signal I g ± 0.02	Signal I ΔH, Oe	Signal II g ± 0.02	Signal II ΔH, Oe	Signal III g ± 0.001	Signal III ΔH, Oe
Al_2O_3 nanopowder produced by laser evaporation	4.27	86	2.33	341	–	–
The same after electron radiation	4.27	81	2.33	254	2.002	38
Al_2O_3 nanopowder produced by explosion	4.27	74	2.08	620	–	–
The same after electron radiation	4.27	72	2.06	517	2.006	48
Al_2O_3 nanopowder with 2.5 wt.% TiO_2 produced by explosion	4.27	78	2.05	615	–	–
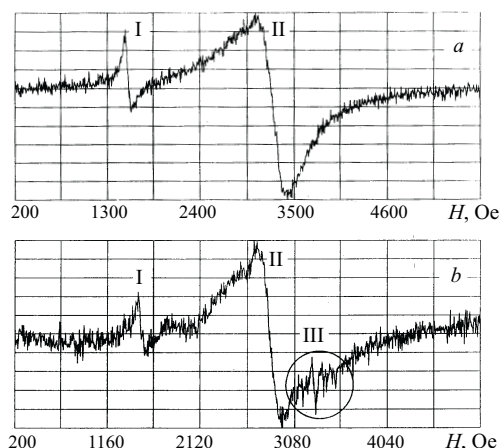
Fig. 1. EPR spectra of Al_2O_3 powders before (*a*) and after (*b*) electron radiation (signal emitted by F^+ center is designated by the circle).

Fig. 2. EPR spectra of ceramics made by sintering Al_2O_3 nanopowder (numbers indicate relative correlations of signal intensities).

constituted a wide intense signal with $g = 2.28 \pm 0.1$ and $\Delta H = 2092 \pm 100$ Oe emitted by Fe^{3+} ions in ferromagnetic oxides of iron. Ferromagnetic oxides $\gamma\text{-}Fe_2O_3$ and Fe_3O_4 and antiferromagnetic compounds exist in the nanopowder as extremely small particles of size ≈ 80 nm. At the same time, they transform into superparamagnetic state, i.e., the particles bind by affinity. Particles of size ≤ 80 nm are capable of forming clusters of the $Fe - O - Fe$ type [5].

Due to the low content of iron oxides in Al_2O_3 nanopowders, it was impossible to identify the phase composition of iron impurities. We believe that iron impurities in Al_2O_3 nanopowders also form $Fe - O - Fe$ clusters, which exist in the supermagnetic state and coat the Al_2O_3 nanocrystals. The width of the signal largely depends on the cluster structure and is presumably determined by the length of the $Fe - O - Fe$ chains (dimers or trimers). This can account for the significant narrowing of the signal from Fe^{3+} ions in the nanopowder produced by laser beam evaporation of aluminum oxide ceramics, as compared to the samples produced by explosion.

Another component of signal II is presumably related to the presence of slight impurities of Cr^{3+} ions in the samples. The presence of chromium oxide impurities in Al_2O_3 nanopowders produced by different methods is indicated by the x-ray luminescence data. It is found that nanopowders of both types under the effect of x-radiation luminesce in the green range (with a maximum at $510 - 530$ nm), which corresponds to the luminescence of a chromium oxide phase (probably Cr_2O_3). The presence of chromium oxide in aluminum ceramics is a known fact [6]. In production by explosion, in spite of the fact that chromium impurities were not identified in the initial aluminum wire, chromium can penetrate into Al_2O_3 nanopowder in the course of production. The explosion chamber is made of stainless steel, and Al_2O_3 nanopowder, which is very hard, can grate metallic chromium in the chamber. The computer analysis of signal II
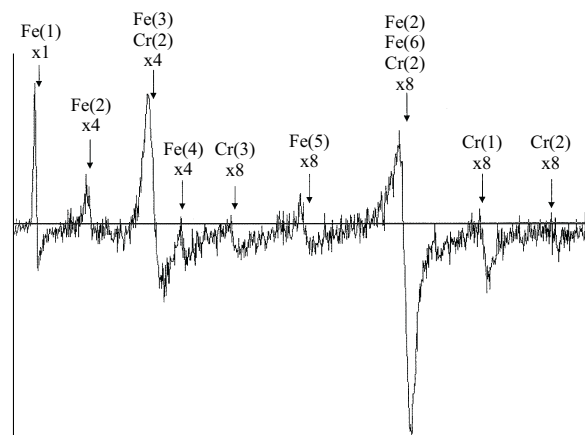
made it possible to distinguish in it two lines, one of which has the parameters $g_\parallel = 2.22$ and $g_\perp = 2.38$, and the second line is characterized by a *g*-factor equal to 1.98. Thus, the registered signal II is the superposition of the signals correlated with Fe^{3+} and Cr^{3+} ion impurities.

The electron radiation of Al_2O_3 nanopowder is accompanied by a decrease in the signal amplitude and the band width, which is presumably related to the conversion of part of the Fe^{3+} ions to Fe^{2+} ($Fe^{3+} + \bar{e} = Fe^{2+}$), which cannot be identified by the EPR method at room temperature. It is notable that the radiated samples exhibit a relatively weak signal III (Fig. 1*b*), which is probably determined by F^+ centers that constitute an anion vacancy having trapped an electron [7]. In addition to the stoichiometric Al_2O_3 phase, one can expect the presence in the nanopowder of a metastable aluminum oxide phase which has a shortage of oxygen (anion vacancies). Electron radiation leads to the localization of an electron in the anion vacancy and the formation of a F^+ center.

The TiO_2 nanopowder contains a slight impurity of Ti^{3+} ions (about 10^{15} spin/g). It is impossible to identify the concentration of Ti^{3+} ions in the spectra of the mixture of Al_2O_3 and TiO_2 powders, due to the superposition of the titanium band on the central signal of ferric ions. As a consequence, the nanopowders with titanium impurities have the same paramagnetic signals as pure Al_2O_3.

The EPR spectra of ceramics made by sintering Al_2O_3 nanopowder, both pure and with TiO_2 additives, differ significantly from the initial powder spectra (Fig. 2). The intensity of signals I and II decreases significantly. The spectra exhibit new bands, both in the lower and the higher field (Table 3). The observed modifications in the spectra reflect the substantial modification of the matrix structure in sintering and are presumably related to the fact that iron and chromium ions, which in the nanopowder used to exist in separated phases, in sintering become incorporated in the Al_2O_3 lattice. This assumption is corroborated for chromium ions by the luminescence analysis data. When excited by x-ray ra-

diation, the Al_2O_3 ceramics produced by sintering nano-powders made from aluminum wire luminesced in the red spectrum range (with a maximum at 710 – 730 nm), which is typical of Cr^{3+} ions replacing Al^{3+} ions in the Al_2O_3 cation sublattice (*R*- and *N*-lines).

The EPR spectra start revealing the effects of a fine structure which is not totally averaged, as happens in powders. This is evidence of the fact that the classical powdered state disappears, and the structure consists of grains constituting clusters of microcrystals. The position and intensity of EPR lines belonging to a particular microcrystal in ceramics depend on the angles formed by its symmetry axes and the external magnetic field vector. The observed summary EPR spectrum represents an envelope of all individual lines generated by single microcrystals.

The precise attribution of registered signals is not easy, due to the superposition of the EPR lines of iron and chromium ions and the components of their fine structure. However, it is obvious that the obtained values of the spectroscopic parameters reflect the fact that these ions occupy nonequivalent crystallographic positions. Signal (4), as in nanopowders, belongs to the Fe^{3+} ion in the orthorhombic crystal field of α-Al_2O_3. Signal (5) is described in the literature [4] as related to Fe^{3+} in the cubic crystal field which is typical of the solid solution of Fe_2O_3 in γ-Al_2O_3 at $2D > h\nu$. It is known as well that in the presence of a strong axial field at $|D| \gg h\nu$ and $E = 0$, the Fe^{3+} signal with $g_\perp \approx 6$ and $g_\parallel \approx 2$ was detected in glasses [8]. We believe that signal (2) observed by us also belongs to iron ions in a strong axial field. The parallel orientation of this signal is superimposed on the signal with $g = 2.04$, which was observed in the powders. The presence of the signal with $g = 2.04$ is probably related to the fact that a small fraction of iron ions is preserved in the form of clusters at the borders of microcrystals and grains. Line (1) in the lower field corresponding to $g \approx 16$ may be related to Fe^{3+} ions in the orthorhombic field, which are associated with negatively charged defects [9]. Such a position of iron ions in ceramics is preferable, since signal (1) has the highest intensity.

The other lines in the spectrum are generated by Cr^{3+} ions which, as iron ions, exist in different crystallographic positions. Signal (1) is related to the ions of chromium in the axial crystalline field, and signals (2) and (3) are related to Cr^{3+} in the octahedral field with a strong axial and orthorhombic distortion, whereas for signal (3), $E \gg D$ [8].

The EPR signal of Ti^{3+} impurity ions is absent from ceramics produced by the sintering of nanopowders with TiO_2 additive, which is due to the complete oxidation of titanium (to Ti^{4+}). After electron radiation of ceramics, the EPR spectra remain unchanged, which points to the absence of oxygen vacancies.

Thus, the EPR method was used to study the defect structure of aluminum oxide nanopowders and ceramics based on these powders. The study identified inherent structural point defects in nanopowders, which are oxygen vacancies having a trapped electron (F^+ centers). Such F^+ centers are absent in ceramics. Among the impurity defects in nanopowders and ceramics, signals from Fe^{3+}, Cr^{3+}, and Ti^{3+} ions were identified, which occupy different crystallographic positions in Al_2O_3 or exist as separate phases.

REFERENCES

1. I. A. Gusev, *Nanocrystalline Materials: Production Methods and Properties* [in Russian], Izd. UrO RAN, Ekaterinburg (1998).
2. Y. A. Kotov, J. V. Beketov, A. M. Murzakaev, et al., "Synthesis of Al_2O_3, TiO_2, and ZrO_2 nanopowders by electrical explosion of wires," in: *Materials Science Forum, Vol. 225, Part 2*, Switzerland (1996), pp. 913 – 916.
3. V. V. Ivanov, *Production of Nanostructural Ceramics Using Magnetic-Pulse Compression of Powders, Author's Abstract of Doctoral Thesis* [in Russian], Ekaterinburg (1998).
4. F. Gesmundo and C. Asmundis, "An EPR Study of Solid Solutions of Ferric Oxide in γ-Al_2O_3," *Phys. Chem. Solids*, **35**(8), 1007 – 1013 (1974).
5. I. A. Ivan'kin, *The State of Iron and Manganese Ions in Raw Materials and Clinker and Their Effect on the Pigmentation of White Cement, Author's Abstract of Candidate's Thesis* [in Russian], Sverdlovsk (1990).
6. N. M. Pavlushkin, *Sintered Corundum* [in Russian], Stroiizdat, Moscow (1961).
7. A. S. Marfunin, *Spectroscopy, Luminescence, and Radiation Centers in Minerals* [in Russian], Nedra, Moscow (1975).
8. S. A. Al'tshuler and B. M. Kozyrev, *Electron Paramagnetic Resonance of Intermediate Group Compounds* [in Russian], Nauka, Moscow (1972).
9. K. Morigaki and T. Hoshina, "Electron spin resonance of Fe^{3+} associated centres in cadmium selenide," Techn. Rept. ISSP, **A**(253), 21 – 27 (1967).